

Probing uncertainties of nuclear structure corrections in light muonic atoms

O. J. Hernandez^{a,b}, C. Ji^{c,*}, S. Bacca^a, and N. Barnea^d

^a *Institut für Kernphysik and PRISMA Cluster of Excellence,
Johannes Gutenberg-Universität Mainz,
55128 Mainz, Germany*

^b *Department of Physics and Astronomy,
University of British Columbia,
Vancouver, BC, V6T 1Z4, Canada*

^c *Key Laboratory of Quark and Lepton Physics (MOE) and Institute of Particle Physics,
Central China Normal University, Wuhan 430079, China*

^d *Racah Institute of Physics,
The Hebrew University, Jerusalem 91904, Israel*

Recent calculations of nuclear structure corrections to the Lamb shift in light muonic atoms are based on an expansion in a parameter η , where only terms up to second order are retained. The parameter η can be shown to be proportional to $\sqrt{m_r/m_p}$, where m_r is the reduced mass of the muon–nucleus system and m_p is the proton mass, so that it is small and the expansion is expected to converge. However, practical implementations show that the η convergence may be slower than expected. In this work we probe the uncertainties due to this expansion using a different formalism, which is based on a multipole expansion of the longitudinal and transverse response functions and was first introduced by Leidemann and Rosenfelder [1, 2]. We refer to this alternative expansion as the η -less formalism. We generalize this formalism to account for the cancellation of elastic terms such as the third Zemach moment (or Friar moment) and embed it in a computationally efficient framework. We implement and test this approach in the case of muonic deuterium. The comparison of results in the point nucleon limit for both methods achieve sub-percent agreement. When nucleon form factors are introduced we find a 4% and 2% difference in the third Zemach moment and nuclear polarizability, respectively, compared to the η -less expansion, indicating that the nucleon form factor approximations in Ref. [3] should be improved. However, we find that the sum of these terms removes this dependence and the uncertainty due to the η -expansion and the related second-order approximation in the nucleon form factors amounts only to 0.2% and thus is fully justified in muonic deuterium. This computationally efficient framework paves the way to further studies in light muonic systems with more than two nucleons, where controlling and reducing uncertainties in nuclear structure corrections is key to the experimental efforts of the CREMA collaboration.

PACS numbers: 21.10.Ky, 23.20.-g, 23.20.Js, 27.20.+n

I. INTRODUCTION

Light muonic atoms have attracted a lot of attention in recent years. The discovery of the proton radius puzzle [4, 5] and the subsequent deuteron radius puzzle [6] have driven the experimental effort to probe the Lamb shift in heavier muonic atoms, such as muonic helium, and possibly muonic lithium in the future [7]. The Lamb shift δ_{LS} is related to the charge radius of a nucleus r_{nuc} by

$$\delta_{\text{LS}} = \delta_{\text{QED}} + \mathcal{A}_{\text{OPE}} r_{\text{nuc}}^2 + \delta_{\text{TPE}}. \quad (1)$$

The term δ_{QED} denotes the quantum electrodynamics (QED) corrections dominated by the vacuum-polarization and self-energy effects of the muon. The next two terms, $\mathcal{A}_{\text{OPE}} r_{\text{nuc}}^2$ and δ_{TPE} , are the nuclear structure corrections stemming from one- and two-photon exchange (TPE), respectively. The values of

δ_{QED} , \mathcal{A}_{OPE} , and δ_{TPE} in Eq. (1) need to be provided by theory and are key to extract the radius r_{nuc}^2 from a spectroscopic measurement of the Lamb shift. For muonic atom experiments, δ_{TPE} is the bottleneck in the exploitation of the experimental precision and its uncertainty drives the precision by which the radius can be extracted from Eq. (1). By convention, δ_{TPE} is evaluated as a sum of terms that depend on dynamics of the atomic nucleus and the nucleon, denoted with an A and N , respectively. These terms are further broken up into the elastic Zemach component ($\delta_{\text{Zem}}^{A/N}$) and the inelastic polarizability contribution ($\delta_{\text{pol}}^{A/N}$), so that

$$\delta_{\text{TPE}}^{A/N} = \delta_{\text{Zem}}^{A/N} + \delta_{\text{pol}}^{A/N}. \quad (2)$$

The elastic contributions are embodied by the third Zemach moment [8] (or Friar moment [9]) and are thus denoted with the label “Zem”.

For muonic deuterium (μD), the TPE contributions δ_{TPE} have been calculated by several independent theoretical works [10–15]. In the μD experiment, the CREMA

* jichen@mail.cnu.edu.cn

collaboration determination of the deuteron charge radius [6] deviates by 5.6σ with respect to the CODATA-2014 evaluation [16]. Another less significant difference in the deuteron was found between the experimentally extracted muonic isotope-shift radius and the electronic one $r_D^2 - r_p^2$ [6, 17]. A thorough analysis of all systematic and statistical uncertainties in the theoretical calculations of δ_{TPE} was carried out in Ref. [15] and could not account for the deuteron radius puzzle or the smaller isotope-shift disagreement. In that work, the TPE contributions at fifth order in α were calculated which also included the logarithmic Coulomb corrections at order $\alpha^6 \ln \alpha$. The uncertainty arising from other uncalculated α^6 diagrams were estimated. These estimates were consistent with the work of Ref. [18] where the three-photon exchange contributions were calculated. However, recent work by Kalinowski [19] has found that the effect of the vacuum polarization in μD of order α^6 was larger than expected and shifted the central value of δ_{TPE} towards the experiment. It remains an open question to demonstrate that a consistent calculation of all other relevant contributions at α^6 order are as negligible as expected.

In the work of Refs. [10–13, 20, 21] the nuclear polarizability corrections originating from the TPE were calculated by a multipole expansion of the operator $\eta = \sqrt{2m_r\omega_N}|\mathbf{R}-\mathbf{R}'|$, where m_r is the reduced lepton-nuclear mass, ω_N is the nuclear excitation energy and $|\mathbf{R}-\mathbf{R}'|$ is the “virtual” distance that a nucleon travels inside the nucleus during the TPE process. The nuclear excitation energy is of the order $\omega_N \sim Q^2/(2m_p)$ where m_p is the proton mass and Q is the momentum of the moving proton. Based on the uncertainty principle $Q \sim 1/|\mathbf{R}-\mathbf{R}'|$, one can see that $\eta \sim \sqrt{m_r/m_p}$, and therefore η is expected to be small. This theoretical formalism referred to as the “ η -expansion”, will be briefly reviewed in the next section.

The η -expansion is useful for obtaining closed form expressions that can be easily computed. It can also be used to extract elastic contributions from δ_{pol}^A that cancel corresponding terms from the elastic TPE. However, for this η -expansion method to be valid and accurate, the parameter η must be much smaller than 1. For the muonic deuterium and helium-4 the expansion was observed to converge quickly [12, 20, 21]. However, for the muonic tritium and helium-3 the η -expansion was observed to converge slowly [22, 23], leading to a larger estimated truncation uncertainty from this method.

Extending the η -expansion to higher orders is technically complicated and motivates us to investigate the more systematic framework introduced by Leidemann and Rosenfelder [1, 2] for calculating the TPE, which will be referred to as the “ η -less” method in this paper. Leidemann and Rosenfelder’s method has not been used in recent calculations of the nuclear TPE due to its higher computational complexity. Furthermore, the original formulation did not allow the extraction of the elastic terms from the polarizability contribution, thus did not exploit direct cancellations of the Zemach mo-

ments [10, 11]. In this work, we revisit the original Leidemann and Rosenfelder formalism and show that the Lanczos sum rule method [24] can be adapted to tackle these calculations. We also establish how the elastic term implicitly contained in the polarizability can be extracted and removed for any general TPE diagram.

We apply our new formalism to μD , and compare it with the η -expansion method. To this end we utilize two nuclear force models. We first use nuclear potentials from pionless effective field theory (πEFT) at next-to-next-to-leading order [11]. This allows for the derivation of analytic results that are used as a benchmark between η -less and η -expansion calculations. Next we use nucleon-nucleon potentials derived from chiral effective field theory (χEFT) [25].

The paper is organized as follows. Section II A provides a brief pedagogical overview of the η -expansion and motivates the alternative η -less formalism for the non-relativistic case, followed by Section II B that introduces the covariant formalism of Ref. [1, 2] and generalizes the η -less expansion. In Section II C, we outline how the elastic terms that are implicitly included in the η -less formalism can be extracted from the inelastic TPE diagram. The latter will partially cancel the contributions from the elastic two-photon diagrams. Finally, in Section IV we present the results of this formalism for muonic deuterium, compare them against the results from η -expansion and discuss future extensions of the work to other muonic atoms. The details of the πEFT calculations are given in Appendix A, corrections from finite nucleon size effects are explained in Appendix B and the details of the multipole expansion in η -less formalism are in Appendix C.

II. THEORETICAL FRAMEWORK

A. The η -expansion

In the work of Refs. [3, 10, 11, 15, 20, 24] the nuclear polarizability contributions were derived from a power expansion of the small parameter η . In this section we briefly review this approach.

The non-relativistic limit of the nuclear polarizability $\delta_{\text{pol}}^{\text{NR}}$ can be calculated from the second order perturbation theory through the matrix element [3]

$$\delta_{\text{pol}}^{\text{NR}} = \langle N_0\mu | \Delta H G \Delta H | N_0\mu \rangle, \quad (3)$$

where $|\mu N_0\rangle = |\mu\rangle \otimes |N_0\rangle$ is the outer product of the nuclear ground state $|N_0\rangle$ and the muon $2S$ -state wave function $|\mu\rangle$. The operator G is the inelastic Green’s function of the Hamiltonian, $H = H_{\text{nuc}} + H_\mu$, where H_μ is the muon Hamiltonian and H_{nuc} is the nuclear one. The nuclear structure perturbs to the point-Coulomb interaction by

$$\Delta H = \sum_a^Z \Delta V(\mathbf{r}, \mathbf{R}_a), \quad (4)$$

where

$$\Delta V(\mathbf{r}, \mathbf{R}_a) = -\alpha \left(\frac{1}{|\mathbf{r} - \mathbf{R}_a|} - \frac{1}{r} \right). \quad (5)$$

Here \mathbf{r} is the position of the muon relative to the center of the nucleus, \mathbf{R}_a denotes the coordinates of the a -th proton relative to the nuclear center, α is the fine structure constant and Z is the charge number of the nucleus. Integrating over \mathbf{r} allows Eq. (3) to be re-written in terms of the muon matrix element W as

$$\delta_{\text{pol}}^{\text{NR}} = \sum_{N \neq N_0} \int d^3R d^3R' \rho_N^p(\mathbf{R}) W(\mathbf{R}, \mathbf{R}', \omega_N) \rho_N^p(\mathbf{R}'), \quad (6)$$

where $\rho_N^p(\mathbf{R})$ is the nuclear point-proton transition density, which is defined by

$$\rho_N^p(\mathbf{R}) = \langle N | \frac{1}{Z} \sum_a^Z \delta(\mathbf{R} - \mathbf{R}_a) | N_0 \rangle. \quad (7)$$

The muon matrix element can be written as

$$W(\mathbf{R}, \mathbf{R}', \omega_N) = -Z^2 |\phi_\mu(0)|^2 \int \frac{d^3q}{(2\pi)^3} \left(\frac{4\pi\alpha}{q^2} \right)^2 \times (1 - e^{i\mathbf{q}\cdot\mathbf{R}}) \frac{1}{\frac{q^2}{2m_r} + \omega_N} (1 - e^{-i\mathbf{q}\cdot\mathbf{R}'}), \quad (8)$$

with $|\phi_\mu(0)|^2 = (m_r Z \alpha)^3 / 8\pi$ denoting the norm of the muon $2S$ wave function. After carrying out the integral over the momentum \mathbf{q} of the virtual photon, W becomes a function of the dimensionless parameter $\eta = \sqrt{2m_r \omega_N} |\mathbf{R} - \mathbf{R}'|$

$$W(\mathbf{R}, \mathbf{R}', \omega_N) = -\frac{\pi}{m_r^2} (Z\alpha)^2 |\phi_\mu(0)|^2 \left(\frac{2m_r}{\omega_N} \right)^{3/2} \times \frac{1}{\eta} \left(e^{-\eta} - 1 + \eta - \frac{1}{2}\eta^2 \right). \quad (9)$$

As discussed in the introduction, this dimensionless parameter has been qualitatively argued to be of the order $\sqrt{\frac{m_\mu}{m_p}} < 1$ allowing W to be expanded in powers of η .

This η -expansion allows the non-relativistic expression to be a sum of leading, subleading, etc., contributions with respect to the associated powers of η

$$\delta_{\text{pol}}^{\text{NR}} = \delta_{\text{NR}}^{(0)} + \delta_{\text{NR}}^{(1)} + \delta_{\text{NR}}^{(2)} + \dots, \quad (10)$$

where $\delta_{\text{NR}}^{(0)}$ is dominated by the dipole correction $\delta_{D1}^{(0)}$ [3], and the sub-leading term $\delta_{\text{NR}}^{(1)}$ is the sum of the elastic contributions $\delta_{R3}^{(1)}$ and $\delta_{Z3}^{(1)}$ [3] with

$$\delta_{R3}^{(1)} = -\frac{\pi}{3} m_r (Z\alpha)^2 |\phi_\mu(0)|^2 \times \iint d^3R d^3R' |\mathbf{R} - \mathbf{R}'|^3 \rho_0^{(pp)}(\mathbf{R}, \mathbf{R}'), \quad (11)$$

and

$$\delta_{Z3}^{(1)} = \frac{\pi}{3} m_r (Z\alpha)^2 |\phi_\mu(0)|^2 \times \iint d^3R d^3R' |\mathbf{R} - \mathbf{R}'|^3 \rho_0^p(\mathbf{R}) \rho_0^p(\mathbf{R}'), \quad (12)$$

where ρ_0^p is the ground state point-proton density and $\rho_0^{(pp)}$ denotes the proton-proton correlation density. It is important to note that the latter term exactly cancels out the elastic contribution δ_{Zem}^A , i.e., $\delta_{Z3}^A = -\delta_{Zem}^A$ in Eq. (2). In the work of [3, 10–13, 20, 22], the η -expansion was carried out up to sub-sub-leading order. Higher order terms in this expansion lead to non-analytic expressions that are difficult to calculate and have until now only been estimated [3, 10].

The η -expansion can be circumvented by introducing the multipole expansion of $\exp(i\mathbf{q}\cdot\mathbf{R})$ into Eq. (8), integrating over the angles \hat{q} and plugging the result back into Eq. (6). This results in the TPE correction

$$\delta_{\text{pol}}^{\text{NR}} = -8(Z\alpha)^2 |\phi_\mu(0)|^2 \int_0^\infty dq \int_{\omega_{\text{th}}}^\infty d\omega K_{\text{NR}}(q, \omega) S_L(q, \omega), \quad (13)$$

where the non-relativistic Kernel is defined as

$$K_{\text{NR}}(q, \omega) = \frac{1}{q^2 \left(\frac{q^2}{2m_r} + \omega \right)}, \quad (14)$$

and S_L is the longitudinal nuclear response function defined in the next section. The expression in Eq. (13) provides a more systematic method to calculate the nuclear structure corrections, however, it is not apparent that it contains the elastic term $\delta_{Z3}^{(1)}$ that cancels the corresponding term from the elastic diagram. Nonetheless, as we shall demonstrate in Section II C the extraction of the elastic components of a general TPE diagram can be readily accomplished by generalizing the formalism of Refs. [1, 2] discussed in the next section.

B. η -less formalism

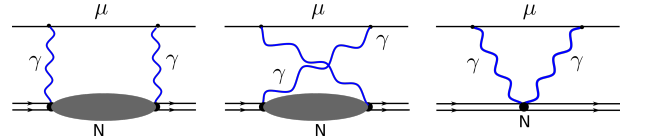


FIG. 1. Two-photon exchange diagrams: direct, crossed and seagull diagrams. The grey blob represents the excited states of the nucleus.

Following the work in Refs. [1, 2], the contributions of the TPE diagrams given by Fig. 1 are

$$\delta_{\text{pol}}^A = -8(Z\alpha)^2 |\phi_\mu(0)|^2 \text{Im} \int \frac{d^4p}{(2\pi)^4} D^{\mu\rho}(p) D^{\nu\tau}(-p) \times t_{\mu\nu}(p, k) T_{\rho\tau}(p, -p), \quad (15)$$

where $D^{\mu\nu}(p)$ is the photon propagator, $t_{\mu\nu}(p, k)$ is the lepton tensor with $k = (m_r, \mathbf{0})$ and $T_{\mu\nu}(p, -p)$ is the hadronic tensor. The evaluation of this amplitude in the Coulomb gauge yields

$$\delta_{\text{pol}}^A = -8(Z\alpha)^2 |\phi_\mu(0)|^2 \int_0^\infty dq \int_{\omega_{\text{th}}}^\infty d\omega [K_L(q, \omega) S_L(q, \omega) + K_T(q, \omega) S_T(q, \omega) + K_S(q, \omega) S_T(0, \omega)], \quad (16)$$

here we integrate over the nuclear excitation energy ω and the magnitude of the three-momentum vector $q = |\mathbf{q}|$. The lower limit ω_{th} in the integral is the nuclear threshold energy. $S_L(q, \omega)$ and $S_T(q, \omega)$ are the longitudinal and transverse response functions, respectively. They are defined as

$$S_L(q, \omega) = \sum_{N \neq N_0} |\langle N | \tilde{\rho}(q) | N_0 \rangle|^2 \delta(\omega_N - \omega), \quad (17)$$

$$S_T(q, \omega) = \sum_{\lambda = \pm 1} \sum_{N \neq N_0} |\langle N | \hat{e}_\lambda^\dagger \cdot \tilde{\mathbf{J}}(q) | N_0 \rangle|^2 \delta(\omega_N - \omega), \quad (18)$$

where $|N_0\rangle$ and $|N\rangle$ are the ground and excited states of the nucleus, with energies E_0 and E_N , respectively. $\omega_N = E_N - E_0$ is the nuclear excitation energy. Here the summation over excited states is averaged over their angular momentum projections. The vectors \hat{e}_λ^\dagger are the circular transverse polarization vectors. The operators $\tilde{\rho}$ and $\tilde{\mathbf{J}}$ are the Fourier transforms of the nuclear charge and current densities, respectively. As in Refs. [1, 2] the kernels in the integrals of Eq. (16) are

$$K_L(q, \omega) = \frac{1}{2E_q} \left[\frac{1}{(E_q - m_r)(\omega + E_q - m_r)} - \frac{1}{(E_q + m_r)(\omega + E_q + m_r)} \right], \quad (19)$$

$$K_T(q, \omega) = \frac{q^2}{4m_r^2} K_L(q, \omega) - \frac{1}{4m_r q} \frac{\omega + 2q}{(\omega + q)^2}, \quad (20)$$

$$K_S(q, \omega) = \frac{1}{4m_r \omega} \left[\frac{1}{q} - \frac{1}{E_q} \right], \quad (21)$$

where $E_q = \sqrt{m_r^2 + q^2}$ is the relativistic energy of the muon. It is convenient to separate the transverse response function into the electric S_T^E and magnetic S_T^M response functions. The nuclear polarization from the TPE is then decomposed into the sum

$$\delta_{\text{pol}}^A = \Delta_L + \Delta_{T,E} + \Delta_{T,M}, \quad (22)$$

where the subscripts L , (T, E) and (T, M) denote the longitudinal, transverse-electric and transverse-magnetic corrections, respectively. These corrections are given ex-

PLICITLY by

$$\Delta_L = -8(Z\alpha)^2 |\phi_\mu(0)|^2 \int_0^\infty dq \int_{\omega_{\text{th}}}^\infty d\omega K_L(q, \omega) S_L(q, \omega), \quad (23)$$

$$\Delta_{T,E} = -8(Z\alpha)^2 |\phi_\mu(0)|^2 \int_0^\infty dq \int_{\omega_{\text{th}}}^\infty d\omega \times [K_T(q, \omega) S_T^E(q, \omega) + K_S(q, \omega) S_T^E(0, \omega)], \quad (24)$$

$$\Delta_{T,M} = -8(Z\alpha)^2 |\phi_\mu(0)|^2 \int_0^\infty dq \int_{\omega_{\text{th}}}^\infty d\omega K_T(q, \omega) S_T^M(q, \omega). \quad (25)$$

In the non-relativistic limit, $q \ll m_r$, the kernels reduce to their non-relativistic forms

$$K_L(q, \omega) \rightarrow K_{\text{NR}}(q, \omega), \quad (26)$$

$$K_T(q, \omega) \rightarrow 0, \quad (27)$$

$$K_S(q, \omega) \rightarrow 0, \quad (28)$$

and Eq. (23) reduces to the expression given by Eq. (13). Eqs. (22-25) summarize the calculation of δ_{pol}^A within the methodology of the η -less expansion.

C. Subtraction of the elastic part

The inelastic TPE calculation in the η -less expansion implicitly contains contributions from terms related to elastic corrections, such as the Zemach moments that cancel out corresponding terms in the elastic TPE diagram. Here we refer to the elastic TPE diagrams as those where the nucleus remains in the ground state throughout the process, while the inelastic diagrams are those in which there is sufficient energy transfer from the virtual photons to excite or breakup the nucleus. A consistent TPE calculation requires the treatment of both terms.

Here we describe how these elastic terms can be extracted directly from the η -less formalism and give the conditions under which there will be a cancellation between the elastic and inelastic contributions for a TPE diagram at order α^5 and higher.

Fig. 2 illustrates the most general elastic and inelastic TPE diagrams, with the light blue square indicating processes that can be inserted into the photon or lepton propagators in the upper half of the diagrams. The contribution of the elastic diagram in Fig. 2a will be denoted as δ_{el}^A , while the inelastic diagram in Fig. 2b is δ_{pol}^A . The contribution from the elastic diagram is

$$\delta_{\text{el}}^A = -8(Z\alpha)^2 |\phi_\mu(0)|^2 \int_0^\infty dq K_{\mu\nu}(q, i0^+) \times \langle N_0 | \tilde{\mathbf{J}}^\mu(q) | N_0 \rangle \langle N_0 | \tilde{\mathbf{J}}^\nu(-q) | N_0 \rangle, \quad (29)$$

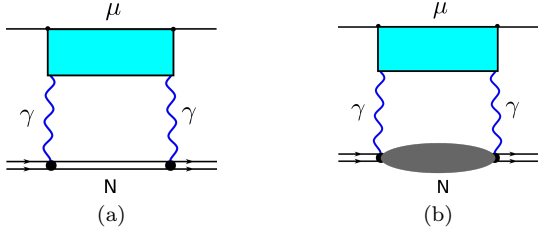


FIG. 2. Two-photon exchange diagrams: (a) elastic vs (b) inelastic. The light blue square represents electromagnetic processes involving the upper half of the diagram. In the inelastic diagram (b) the excited states of the nucleus are represented by the grey blob.

where 0^+ indicates that the $\omega \rightarrow 0^+$ limit is taken. The kernel $K_{\mu\nu}(q, i0^+)$ is determined by the processes considered in the squares of Fig. 2. The matrix elements $\langle N_0 | J^\mu(q) | N_0 \rangle$ represent the elastic electromagnetic vertices of the nucleus in the ground state. The generalized form of Eq. (16) for the inelastic process is

$$\delta_{\text{pol}}^A = -8(Z\alpha)^2 |\phi_\mu(0)|^2 \int_0^\infty dq \int_{\omega_{\text{th}}}^\infty d\omega K_{\mu\nu}(q, \omega) S^{\mu\nu}(q, \omega). \quad (30)$$

The general nuclear response function $S^{\mu\nu}(q, \omega)$ is

$$S^{\mu\nu}(q, \omega) = \sum_{N \neq N_0} \langle N_0 | \tilde{J}^\mu(q) | N \rangle \langle N | \tilde{J}^\nu(-q) | N_0 \rangle \times \delta(\omega_N - \omega). \quad (31)$$

The expression in Eq. (31) contains the electromagnetic matrix elements connecting the ground state $|N_0\rangle$ to the nuclear excited states $|N\rangle$. The analytical terms that cancel corresponding elastic contributions can be extracted from δ_{pol}^A by separating it into the purely ω -dependent ($\Delta_\omega^{\text{inel}}$) terms and ω -independent ($\Delta_\phi^{\text{inel}}$) components as

$$\delta_{\text{pol}}^A = \Delta_\omega^{\text{inel}} + \Delta_\phi^{\text{inel}}. \quad (32)$$

These ω -dependent/independent corrections are given by

$$\Delta_\omega^{\text{inel}} = -8(Z\alpha)^2 |\phi_\mu(0)|^2 \int_0^\infty dq \int_{\omega_{\text{th}}}^\infty d\omega \times [K_{\mu\nu}(q, \omega) - K_{\mu\nu}(q, i0^+)] S^{\mu\nu}(q, \omega), \quad (33)$$

$$\Delta_\phi^{\text{inel}} = -8(Z\alpha)^2 |\phi_\mu(0)|^2 \int_0^\infty dq \int_{\omega_{\text{th}}}^\infty d\omega \times K_{\mu\nu}(q, i0^+) S^{\mu\nu}(q, \omega), \quad (34)$$

respectively. For the ω -independent terms, the kernel $K_{\mu\nu}(q, i0^+)$ can be taken out from the integration over

ω , so that the remaining integral uses the identity

$$\int_{\omega_{\text{th}}}^\infty d\omega S^{\mu\nu}(q, \omega) = \langle N_0 | \tilde{J}^\mu(q) \tilde{J}^\nu(-q) | N_0 \rangle - \langle N_0 | \tilde{J}^\mu(q) | N_0 \rangle \langle N_0 | \tilde{J}^\nu(-q) | N_0 \rangle, \quad (35)$$

where $\langle N_0 | \tilde{J}^\mu(q) \tilde{J}^\nu(-q) | N_0 \rangle$ is the correlation function of the electromagnetic operators and $\langle N_0 | \tilde{J}^\mu(q) | N_0 \rangle$ is directly related to the elastic electromagnetic form factors of the nucleus. Therefore, $\Delta_\phi^{\text{inel}}$ is divided into two terms

$$\Delta_\phi^{\text{inel}} = \Delta_{\text{corr}} - \delta_{\text{el}}^A, \quad (36)$$

where the first term is the correlation term defined by

$$\Delta_{\text{corr}} = -8(Z\alpha)^2 |\phi_\mu(0)|^2 \times \int_0^\infty dq K_{\mu\nu}(q, i0^+) \langle N_0 | \tilde{J}^\mu(q) \tilde{J}^\nu(-q) | N_0 \rangle. \quad (37)$$

The second term in Eq. (36) cancels out exactly Eq. (29). Therefore, when contributions of elastic and inelastic TPE diagrams are added, only the correlation and the ω -dependent ($\Delta_\omega^{\text{inel}}$) contributions remain. One indeed obtains

$$\delta_{\text{pol}}^A + \delta_{\text{el}}^A = \Delta_{\text{corr}} + \Delta_\omega^{\text{inel}}. \quad (38)$$

For the contributions to Lamb shift at order α^5 , δ_{el}^A in Eq. (29) can reduce to the Zemach term δ_{Zem} . This reduction is very general and applies to transitions other than the Lamb shift such as the hyperfine splitting [26, 27]. Here we only demonstrate it in the point-nucleon limit using the η -less formalism. The nuclear response functions, which contribute to the Lamb shift, are the longitudinal and transverse ones defined in Eqs. (17, 18). When taking the limit $\omega \rightarrow i0^+$, the transverse kernel vanishes, and the longitudinal covariant kernel reduces to the non-relativistic one:

$$K_T(q, i0^+) = 0, \quad (39)$$

$$K_L(q, i0^+) = K_{\text{NR}}(q, i0^+) = \frac{2m_r}{(q^2 + i0^+)^2}. \quad (40)$$

Therefore, the only remaining elastic TPE component is

$$\delta_{\text{el}}^A = -16m_r(Z\alpha)^2 |\phi_\mu(0)|^2 \mathcal{P} \int_0^\infty \frac{dq}{q^4} |\langle N_0 | \tilde{\rho}^p(q) | N_0 \rangle|^2 = -\delta_{Z3}^{(1)} = \delta_{\text{Zem}}^{(1)}, \quad (41)$$

where $\delta_{Z3}^{(1)}$, derived in the η -expansion formalism in Eq. (12), cancels exactly the Zemach term in the point-nucleon limit, i.e., $\delta_{\text{Zem}}^{(1)}$. Similarly, the correlation term

yields

$$\begin{aligned} \Delta_{\text{corr}} &= -16m_r(Z\alpha)^2|\phi_\mu(0)|^2 \\ &\times \mathcal{P} \int_0^\infty \frac{dq}{q^4} \langle N_0 | \tilde{\rho}^p(q) \tilde{\rho}^{p,\dagger}(q) | N_0 \rangle \\ &= \delta_{R3}^{(1)}, \end{aligned} \quad (42)$$

where $\delta_{R3}^{(1)}$, given in Eq. (11), is the proton-proton correlation term from the η -expansion. Combining with Eq. (36), the ω -independent nuclear polarizability correction leads to

$$\Delta_\varphi^{\text{inel}} = \delta_{R3}^{(1)} - \delta_{Z\text{em}}^{(1)}. \quad (43)$$

Therefore, the polarizability contribution in the η -less expression in Eq. (38) can be written as

$$\delta_{\text{pol}}^A = \Delta_\omega^{\text{inel}} + \delta_{R3}^{(1)} - \delta_{Z\text{em}}^{(1)}, \quad (44)$$

where $\Delta_\omega^{\text{inel}}$ are the ω -dependent nuclear polarizability corrections. This example establishes how the elastic contributions can be extracted from the η -less expansion formalism. For muonic deuterium or tritium, the correlation term $\delta_{R3}^{(1)} = 0$ since the nucleus has only one proton.

III. NUMERICAL PROCEDURES

In this section we outline the numerical methods used to calculate the nuclear structure corrections in light muonic atoms within the previously outlined framework. The tools needed are the multipole decomposition for the charge and current density operators, followed by the use of the Lanczos sum rule (LSR) method that makes the required calculations amenable to computation.

Using the multipole expansion from Appendix C on the longitudinal and transverse response functions the nuclear structure corrections in Eqs. (23, 24, 25) are calculated as a sum of terms with different photon multiplicities

$$\Delta_x = \sum_{\mathcal{J}=0} \Delta_{\mathcal{J},x}. \quad (45)$$

Here the symbol x denotes $L, (T, E)$ or (T, M) . In the non-relativistic limit, $\Delta_L \rightarrow \delta_{\text{pol}}^{\text{NR}}$ and $\Delta_{T,E/M} \rightarrow 0$. In practice the integrals in Eqs. (23)-(25) are generalized sum rules of the nuclear response function, Eq. (31), given by

$$I = \int_0^\infty dq \int_{\omega_{\text{th}}}^\infty d\omega K_{\mu\nu}(q, \omega) S^{\mu\nu}(q, \omega), \quad (46)$$

with an arbitrary kernel function $K_{\mu\nu}(q, \omega)$. The calculation of this integral requires the diagonalization of

the complete Hamiltonian which is computationally impractical. To render this problem tractable one may use the LSR method [24] to carry out the integral over the nuclear excitation energies ω , followed by a Gaussian quadrature discretization to integrate over q . The LSR method allows for the efficient computation of sum rules by approximating the full $M \times M$ Hamiltonian matrix with a tridiagonal matrix $H_{M'}$ of dimension M' using the recursive Krylov subspace, where M' is determined by the number of Lanczos iterations. In this Lanczos basis, Eq. (46) becomes

$$\begin{aligned} I_{M'} &= \sum_i^{N_q} W_i \langle N_0 | \tilde{J}^{\dagger\mu}(q_i) \tilde{J}^\nu(q_i) | N_0 \rangle \\ &\times \sum_{m \neq 0}^{M'} |U_{m0}|^2 K_{\mu\nu}(q_i, \omega_m). \end{aligned} \quad (47)$$

Here the integral over the nuclear excitation energy ω in Eq. (46) is carried out as a sum rule by integrating over all of the discretized energy states $\omega_m \equiv E_m - E_0$ where E_m is the m -th eigenvalue of $H_{M'}$ and U is the unitary transformation matrix that diagonalizes $H_{M'}$. The points q_i and W_i for $i = 1, \dots, N_q$ are the Gaussian quadrature grid points and weights, respectively, for the momentum integral in Eq. (46). Within the LSR framework, the low-lying eigenstates and spectral moments converge after a relatively small number of Lanczos iterations M' , where M' is typically much smaller than M , i.e., the dimension of the original Hamiltonian, allowing the generalized sum rules to be calculated very efficiently.

A. Implementation

For the deuteron case, the model space is small and it is possible to use the full diagonalization variant of the Hamiltonian when evaluating the sum rules. The two-body system was solved using the truncated harmonic oscillator basis expansion [23]. The integrals over the momentum were carried out over a discrete Gaussian quadrature grid of 100 points up to a maximum q estimated by the ultraviolet cut-off of the oscillator basis $\Lambda_{\text{UV}} \approx \sqrt{(2N_{\text{Max}} + 7)m_N\Omega/\hbar}$, where Ω is the oscillator frequency and N_{Max} is the model space size [28]. This is much less computationally expensive than calculating the full response function on a grid of ω and q as in Refs. [1, 2]. For nuclei heavier than the deuteron, the Lanczos variant of Eq. (47) can be used.

IV. RESULTS

In this section we provide the results of the η -less formalism for muonic deuterium using both \mathcal{N} EFT and χ EFT interactions. The former is calculated analytically and the latter is evaluated numerically. In the text that

follows, the calculated values are quoted to three significant digits. For the analytical $\not\pi$ EFT case, the results in Table I are quoted up to four digits, while for the results with the χ EFT nuclear forces in Tables II-IV we quote the values up to their estimated numerical uncertainty. The sources of numerical uncertainty considered for the χ EFT force calculations are the oscillator frequency $\hbar\Omega$, the model space size N_{Max} , the maximum momentum value q_{max} used in the integration of the responses and the number of quadrature points N_q used in the momentum integrals. For each \mathcal{J} , the total numerical uncertainty is the quadrature sum of these contributions. These numerical uncertainties are the only ones estimated in Tables II-IV.

A. Analytical $\not\pi$ EFT

Before tackling the muonic deuterium calculation with a χ EFT potential, we adapt the formalism of $\not\pi$ EFT at next-to-next-to-leading order to compute the nuclear structure TPE corrections in μ D in the non-relativistic, point-nucleon limit as in Eq. (13).

\mathcal{J}	$\Delta_{L,\mathcal{J}}$	$\delta_{\text{pol}}^{\text{NR}}$
0	-5.559×10^{-2}	-5.559×10^{-2}
1	-1.451	-1.5066
2	-6.455×10^{-2}	-1.5711
3	-1.182×10^{-2}	-1.5830
4	-3.723×10^{-3}	-1.5867
5	-1.545×10^{-3}	-1.5882
6	-7.571×10^{-4}	-1.5890
7	-4.145×10^{-4}	-1.5894
8	-2.457×10^{-4}	-1.5896
9	-1.546×10^{-4}	-1.5898
10	-1.019×10^{-4}	-1.5899
11	-6.972×10^{-5}	-1.5900
12	-4.918×10^{-5}	-1.5900
13	-3.56×10^{-5}	-1.5901
14	-2.631×10^{-5}	-1.5901
15	-1.981×10^{-5}	-1.5901
16	-1.514×10^{-5}	-1.5901
17	-1.174×10^{-5}	-1.5901
18	-9.207×10^{-6}	-1.5901
19	-7.281×10^{-6}	-1.5901
20	-5.822×10^{-6}	-1.5902

TABLE I. The calculated values of the terms $\Delta_{L,\mathcal{J}}$ that contribute to the two-photon exchange in meV at each multipole \mathcal{J} for μ D with $\not\pi$ EFT at next-to-next-to-leading order, and their running sum $\delta_{\text{pol}}^{\text{NR}} = \sum_{K=0}^{\mathcal{J}} \Delta_{L,K}$.

The formulas to carry out this calculation are presented in Appendix A. In Table I, the individual contributions of the term $\Delta_{L,\mathcal{J}}$ for $\mathcal{J} = 0, \dots, 20$ are given along with the running sum $\delta_{\text{pol}}^{\text{NR}} = \sum_{\mathcal{J}=0}^{\mathcal{J}_{\text{max}}} \Delta_{L,\mathcal{J}}$, that quickly saturates to -1.5902 meV. In the η -formalism with $\not\pi$ EFT, $\delta_{\text{pol}}^{\text{NR}} = \delta_{D1}^{(0)} + \delta_{Z3}^{(1)} + \delta_{R2}^{(2)} + \delta_Q^{(2)} + \delta_{D1D3}^{(2)} = -1.590$ meV in the same non-relativistic and point-nucleon limit. These

results agree within 0.01% indicating an excellent agreement between the η -less and η -expansion methods.

B. χ EFT Case

Now we consider the nucleon-nucleon potential derived from χ EFT at next-to-next-to-next-to-leading order [25]. Calculations are performed as in Ref. [15]. We begin with the non-relativistic formalism in Eq. (13) to compute $\delta_{\text{pol}}^{\text{NR}}$. In Table II, each contribution $\Delta_{L,\mathcal{J}}$ is listed from $\mathcal{J} = 0, \dots, 20$ along with the running sum.

\mathcal{J}	$\Delta_{L,\mathcal{J}}$	$\delta_{\text{pol}}^{\text{NR}}$
0	$-6.85620(1) \times 10^{-2}$	$-6.85620(1) \times 10^{-2}$
1	-1.436198(1)	-1.504760(1)
2	$-6.442519(2) \times 10^{-2}$	-1.569185(1)
3	$-1.18696(1) \times 10^{-2}$	-1.581055(1)
4	$-3.7455(2) \times 10^{-3}$	-1.584800(1)
5	$-1.5570(2) \times 10^{-3}$	-1.586357(1)
6	$-7.649(2) \times 10^{-4}$	-1.587122(1)
7	$-4.201(3) \times 10^{-4}$	-1.587542(1)
8	$-2.502(3) \times 10^{-4}$	-1.587793(1)
9	$-1.583(4) \times 10^{-4}$	-1.587951(1)
10	$-1.051(4) \times 10^{-4}$	-1.588056(1)
11	$-7.25(4) \times 10^{-5}$	-1.588128(1)
12	$-5.16(4) \times 10^{-5}$	-1.588180(1)
13	$-3.77(4) \times 10^{-5}$	-1.588218(1)
14	$-2.82(4) \times 10^{-5}$	-1.588246(1)
15	$-2.15(4) \times 10^{-5}$	-1.588267(2)
16	$-1.66(4) \times 10^{-5}$	-1.588284(2)
17	$-1.31(4) \times 10^{-5}$	-1.588297(2)
18	$-1.04(3) \times 10^{-5}$	-1.588308(2)
19	$-8.4(3) \times 10^{-6}$	-1.588316(2)
20	$-6.8(3) \times 10^{-6}$	-1.588323(2)

TABLE II. The calculated values of the terms $\Delta_{L,\mathcal{J}}$ that contribute to the two-photon exchange in meV as a function of the multipole \mathcal{J} using the χ EFT potential for μ D, and their running sum $\delta_{\text{pol}}^{\text{NR}} = \sum_{K=0}^{\mathcal{J}} \Delta_{L,K}$.

From Table II, we have $\delta_{\text{pol}}^{\text{NR}} = -1.588$ meV. The equivalent result in the η -formalism is $\delta_{\text{pol}}^{\text{NR}} = \delta_{D1}^{(0)} + \delta_{Z3}^{(1)} + \delta_{R2}^{(2)} + \delta_Q^{(2)} + \delta_{D1D3}^{(2)} = -1.590$ meV. The difference between these values is 0.002 meV indicating excellent agreement between both methods for μ D. Higher order multipole corrections within the η -expansion formalism for muonic deuterium are thus negligible. Furthermore, we note that only the first few terms $\mathcal{J} = 0, 1, 2, 3$ are needed to reach sub-percentage agreement with the final $\delta_{\text{pol}}^{\text{NR}}$ value.

Next, we consider the evaluation of the relativistic expressions in Eqs. (23-25) in the point-nucleon limits. The individual contributions to the TPE are given in Table III with the final result denoted as $\delta_{\text{pol}}^{\text{R}}$.

In the relativistic and point-nucleon limit, the η -expansion yields $\delta_{\text{pol}}^{\text{R}} = \delta_{D1}^{(0)} + \delta_L^{(0)} + \delta_T^{(0)} + \delta_{Z3}^{(1)} + \delta_{R2}^{(2)} + \delta_Q^{(2)} + \delta_{D1D3}^{(2)} = -1.573$ meV can be compared to the η -less result $\delta_{\text{pol}}^{\text{R}} = \Delta_L + \Delta_{T,E} + \Delta_{T,M} = -1.571$ meV,

\mathcal{J}	$\Delta_{L,\mathcal{J}}$	$\Delta_{T,E,\mathcal{J}}$	$\Delta_{T,M,\mathcal{J}}$	$\delta_{\text{pol}}^{\text{R}}$
0	$-6.71358(1)\times 10^{-2}$	0.0	0.0	$-6.71358(1)\times 10^{-2}$
1	-1.415390(1)	$-1.2570(7)\times 10^{-2}$	$2.8243(2)\times 10^{-3}$	-1.492271(6)
2	$-6.186081(7)\times 10^{-2}$	$1.01894(8)\times 10^{-4}$	$5.197(3)\times 10^{-4}$	-1.553511(6)
3	$-1.113425(2)\times 10^{-2}$	$9.00(1)\times 10^{-6}$	$7.05(3)\times 10^{-5}$	-1.564565(6)
4	$-3.44382(3)\times 10^{-3}$	$2.62(1)\times 10^{-6}$	$1.007(6)\times 10^{-4}$	-1.567906(7)
5	$-1.40260(4)\times 10^{-3}$	$1.34(1)\times 10^{-6}$	$2.40(4)\times 10^{-5}$	-1.569283(7)
6	$-6.7570(4)\times 10^{-4}$	$8.3(2)\times 10^{-7}$	$4.9(1)\times 10^{-5}$	-1.569909(7)
7	$-3.6394(5)\times 10^{-4}$	$5.7(2)\times 10^{-7}$	$1.30(6)\times 10^{-5}$	-1.570259(7)
8	$-2.1261(6)\times 10^{-4}$	$4.2(2)\times 10^{-7}$	$3.0(1)\times 10^{-5}$	-1.570442(7)
9	$-1.3203(7)\times 10^{-4}$	$3.3(2)\times 10^{-7}$	$8.2(6)\times 10^{-6}$	-1.570565(7)
10	$-8.605(8)\times 10^{-5}$	$2.6(2)\times 10^{-7}$	$2.0(2)\times 10^{-5}$	-1.570631(7)
11	$-5.830(9)\times 10^{-5}$	$2.1(2)\times 10^{-7}$	$5.5(6)\times 10^{-6}$	-1.570684(7)
12	$-4.08(1)\times 10^{-5}$	$1.7(2)\times 10^{-7}$	$1.4(2)\times 10^{-5}$	-1.570710(7)
13	$-2.93(1)\times 10^{-5}$	$1.4(2)\times 10^{-7}$	$3.9(6)\times 10^{-6}$	-1.570736(7)
14	$-2.16(1)\times 10^{-5}$	$1.2(2)\times 10^{-7}$	$1.0(2)\times 10^{-5}$	-1.570747(7)
15	$-1.62(1)\times 10^{-5}$	$1.0(2)\times 10^{-7}$	$2.9(5)\times 10^{-6}$	-1.570760(7)
16	$-1.24(1)\times 10^{-5}$	$9(2)\times 10^{-8}$	$7(2)\times 10^{-6}$	-1.570765(8)
17	$-9.6(1)\times 10^{-6}$	$7(2)\times 10^{-8}$	$2.2(4)\times 10^{-6}$	-1.570773(8)
18	$-7.5(1)\times 10^{-6}$	$6(2)\times 10^{-8}$	$6(1)\times 10^{-6}$	-1.570775(8)
19	$-6.0(1)\times 10^{-6}$	$5(2)\times 10^{-8}$	$1.7(3)\times 10^{-6}$	-1.570779(8)
20	$-4.8(1)\times 10^{-6}$	$5(2)\times 10^{-8}$	$4(1)\times 10^{-6}$	-1.570779(8)

TABLE III. The calculated values of the terms that contribute to $\delta_{\text{pol}}^{\text{R}}$ in meV as a function of the multipole \mathcal{J} for the χEFT potential. $\delta_{\text{pol}}^{\text{R}} = \sum_{K=0}^{\mathcal{J}} (\Delta_{L,K} + \Delta_{T,E,K} + \Delta_{T,M,K})$ is presented by the running sum.

and amounts to a difference of 0.1%. In the low- q limit the term $\Delta_{T,E,\mathcal{J}=1} = -1.257\times 10^{-2}$ meV corresponds to the relativistic electric transverse polarization $\delta_T^{(0)} = -1.248\times 10^{-2}$ meV from the η -expansion [3] and are in close agreement. The relativistic longitudinal polarizability correction in the η -expansion, $\delta_L^{(0)} = 2.913\times 10^{-2}$ meV, is formally related to the difference between the relativistic and non-relativistic results $\Delta_{L,\mathcal{J}=1}$ in Tables III and II amounting to 2.081×10^{-2} meV. The difference between these results is accounted for by the fact that in the η -expansion formalism, the response function is approximated in the low- q limit, while here we have treated the response functions with the full q dependence.

We proceed to use the relativistic kernels with nucleon form factors. The parametrizations of the electric and magnetic nucleon elastic form factors are

$$G_E^p(q^2) = \frac{1}{(1 + q^2/\beta^2)^2}, \quad (48)$$

$$G_E^n(q^2) = \frac{\lambda q^2}{(1 + q^2/\beta^2)^3}, \quad (49)$$

and

$$G_M^{p/n}(q^2) = \mu_N g_{p/n} G_E^p(q^2), \quad (50)$$

where $\beta^2 = 12/r_p^2$, $\lambda = -r_n^2/6$, $r_n^2 = -0.1161(22)$ fm² and $r_p = 0.84087(39)$ fm are parameters given in Refs. [3, 29]. The magnetic g factors of the proton and neutron are $g_p=5.585694702(17)$ and $g_n=-3.82608545(90)$, respectively, while μ_N is the nuclear magneton.

In the η -formalism of Ref. [3], nucleon size effects were included by approximating the nucleon form factors in Eq. (48) and (49) to linear order in q^2 . This approximation is valid in the η -expansion framework, but diverges in the η -less formalism. Therefore, we carried out the η -less calculations using the full form factors. This result including relativistic effects and nucleon form factors is denoted as δ_{pol}^A and are given in Table IV.

In Table IV the inclusion of nucleon form factors reduces the magnitude of the individual contributions to δ_{pol}^A with respect to Table III in the point-nucleon limit. This is expected because the nucleon form factors suppress the strength of the response functions at high q -values. The total sum of all contributions in Table IV is $\delta_{\text{pol}}^A = -1.531$ meV.

The convergence of $\Delta_L, \Delta_{T,\text{el}}, \Delta_{T,\text{mag}}$ is shown in Figs. 3 and 4 by the decrease of the magnitudes of $\Delta_L, \Delta_{T,E,\mathcal{J}}, \Delta_{T,M,\mathcal{J}}$ with increasing photon multipoles \mathcal{J} . The inclusion of nucleon form factors results in a staggering convergence pattern. This behaviour can be understood by the following argument. The Coulomb multipole tensor operator for the deuteron is

$$C_{\mathcal{J}}(q) = \frac{1}{2} [1 + (-1)^{\mathcal{J}}] j_{\mathcal{J}} \left(\frac{qr}{2} \right) Y^{\mathcal{J}}(\hat{r}) + \frac{1}{2} [\tau_1^3 + (-1)^{\mathcal{J}} \tau_2^3] j_{\mathcal{J}} \left(\frac{qr}{2} \right) Y^{\mathcal{J}}(\hat{r}). \quad (51)$$

where $j_{\mathcal{J}}$ is the spherical bessel function and $\tau_{1/2}^3$ is the third component of the isospin for nucleons 1 and 2, respectively. When acting on the deuteron ground state, ($T_0 = 0, M_{T_0} = 0, S_0 = 1, J_0 = 1, L_0 = 0/2$), the reduced matrix elements for the even multipoles are isoscalar op-

\mathcal{J}	$\Delta_{L,\mathcal{J}}$	$\Delta_{T,E,\mathcal{J}}$	$\Delta_{T,M,\mathcal{J}}$	δ_{pol}^A
0	$-6.27430(1) \times 10^{-2}$	0.0	0.0	$-6.27430(1) \times 10^{-2}$
1	-1.389312(1)	$-1.2729(8) \times 10^{-2}$	$2.7400(2) \times 10^{-3}$	-1.462044(7)
2	$-5.687366(7) \times 10^{-2}$	$9.42909(5) \times 10^{-5}$	$3.7810338(1) \times 10^{-4}$	-1.518446(7)
3	$-8.66690(1) \times 10^{-3}$	$5.6589911(7) \times 10^{-6}$	$3.4725465(8) \times 10^{-5}$	-1.527072(7)
4	$-2.499426(5) \times 10^{-3}$	$1.189995(1) \times 10^{-6}$	$3.046054(2) \times 10^{-5}$	-1.529540(7)
5	$-7.91031(2) \times 10^{-4}$	$3.379354(4) \times 10^{-7}$	$5.54470(1) \times 10^{-6}$	-1.530325(7)
6	$-3.73996(1) \times 10^{-4}$	$1.83995(1) \times 10^{-7}$	$7.40018(2) \times 10^{-6}$	-1.530692(7)
7	$-1.467700(5) \times 10^{-4}$	$7.10098(2) \times 10^{-8}$	$1.67017(1) \times 10^{-6}$	-1.530837(7)
8	$-8.89794(3) \times 10^{-5}$	$5.39528(9) \times 10^{-8}$	$2.56595(3) \times 10^{-6}$	-1.530923(7)
9	$-3.81065(2) \times 10^{-5}$	$2.25638(2) \times 10^{-8}$	$6.4689(1) \times 10^{-7}$	-1.530960(7)
10	$-2.72129(1) \times 10^{-5}$	$2.05594(9) \times 10^{-8}$	$1.06086(4) \times 10^{-6}$	-1.530986(7)
11	$-1.211088(8) \times 10^{-5}$	$8.7809(2) \times 10^{-9}$	$2.8741(1) \times 10^{-7}$	-1.530998(7)
12	$-9.77783(7) \times 10^{-6}$	$9.0617(9) \times 10^{-9}$	$4.8931(4) \times 10^{-7}$	-1.531008(7)
13	$-4.41778(4) \times 10^{-6}$	$3.8693(2) \times 10^{-9}$	$1.3972(1) \times 10^{-7}$	-1.531012(7)
14	$-3.93714(4) \times 10^{-6}$	$4.3939(7) \times 10^{-9}$	$2.4379(3) \times 10^{-7}$	-1.531016(7)
15	$-1.78341(2) \times 10^{-6}$	$1.8585(2) \times 10^{-9}$	$7.2510(8) \times 10^{-8}$	-1.531017(7)
16	$-1.72722(2) \times 10^{-6}$	$2.2826(5) \times 10^{-9}$	$1.2879(3) \times 10^{-7}$	-1.531019(7)
17	$-7.7872(1) \times 10^{-7}$	$9.523(1) \times 10^{-10}$	$3.9588(6) \times 10^{-8}$	-1.531020(7)
18	$-8.1058(1) \times 10^{-7}$	$1.2503(4) \times 10^{-9}$	$7.129(2) \times 10^{-8}$	-1.531020(7)
19	$-3.62163(8) \times 10^{-7}$	$5.134(1) \times 10^{-10}$	$2.2520(5) \times 10^{-8}$	-1.531021(7)
20	$-4.01814(8) \times 10^{-7}$	$7.145(2) \times 10^{-10}$	$4.101(2) \times 10^{-8}$	-1.531021(7)

TABLE IV. The calculated values of the terms that contribute to δ_{pol}^A in meV as a function of the multipole \mathcal{J} for the χ EFT potential. $\delta_{\text{pol}}^A = \sum_{K=0}^{\mathcal{J}} (\Delta_{L,K} + \Delta_{T,E,K} + \Delta_{T,M,K})$ is presented by the running sum.

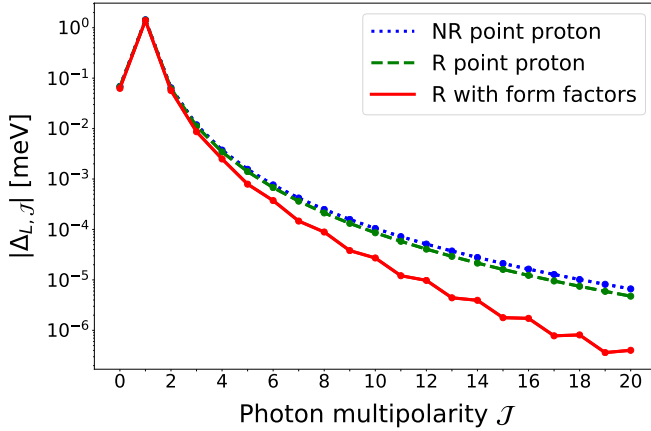


FIG. 3. The absolute value of the longitudinal corrections in the non-relativistic (NR) point-nucleon limit, in the relativistic (Rel) point-nucleon limit, and with nucleon form factors as a function of the multipolarity \mathcal{J} .

erators, while odd multipoles of this operator are isovector transitions

$$\begin{aligned} & \langle J; T, M_T | C_{2\mathcal{J}}(q) | J_0; 0, 0 \rangle \\ &= \langle J | j_{2\mathcal{J}} \left(\frac{qr}{2} \right) Y^{2\mathcal{J}}(\hat{r}) | J_0 \rangle \delta_{T,0} \delta_{m_T,0}, \end{aligned} \quad (52)$$

$$\begin{aligned} & \langle J; T, M_T | C_{2\mathcal{J}+1}(q) | J_0; 0, 0 \rangle \\ &= \langle J | j_{2\mathcal{J}+1} \left(\frac{qr}{2} \right) Y^{2\mathcal{J}+1}(\hat{r}) | J_0 \rangle \delta_{T,1} \delta_{m_T,0}. \end{aligned} \quad (53)$$

The above reduced matrix elements give similar numerical results accounting for the smooth convergence pattern

in Fig. 3 for the point-proton limit. When nucleon form factors are introduced, the matrix elements become

$$\begin{aligned} & \langle J; T, M_T | C_{2\mathcal{J}}(q) | J_0; 0, 0 \rangle \\ &= [G_E^p(q^2) + G_E^n(q^2)] \langle J | j_{2\mathcal{J}} \left(\frac{qr}{2} \right) Y^{2\mathcal{J}}(\hat{r}) | J_0 \rangle \\ & \quad \times \delta_{T,0} \delta_{m_T,0}, \end{aligned} \quad (54)$$

for the even Coulomb multipoles, while the matrix elements of the odd Coulomb multipoles are

$$\begin{aligned} & \langle J; T, M_T | C_{2\mathcal{J}+1}(q) | J_0; 0, 0 \rangle \\ &= [G_E^p(q^2) - G_E^n(q^2)] \langle J | j_{2\mathcal{J}+1} \left(\frac{qr}{2} \right) Y^{2\mathcal{J}+1}(\hat{r}) | J_0 \rangle \\ & \quad \times \delta_{T,1} \delta_{m_T,0}. \end{aligned} \quad (55)$$

The addition between q -dependent proton and neutron form factors enhances the value of $\Delta_{L,\mathcal{J}}$ with an even \mathcal{J} with respect to the one with an odd \mathcal{J} . The enhancement becomes more pronounced at larger even values of \mathcal{J} , and is observed in Fig. 3 and Fig. 4a.

A similar pattern is observed in Fig. 4b, however, in this case it is not due to the inclusion of nucleon form factors, but to the fact that for even \mathcal{J} values, the deuteron transitions are dominated by isovector-spin preserving transitions while odd \mathcal{J} values are dominated by isovector-spin changing operators that are suppressed relative to the former transitions.

The final results for δ_{pol}^A along with the results in the non-relativistic point proton limit $\delta_{\text{pol}}^{\text{NR}}$ and in the relativistic point proton limit $\delta_{\text{pol}}^{\text{R}}$ are given in Table V in comparison to the η -expansion values. We observe that in both the non-relativistic and relativistic cases, δ_{Zem}^A

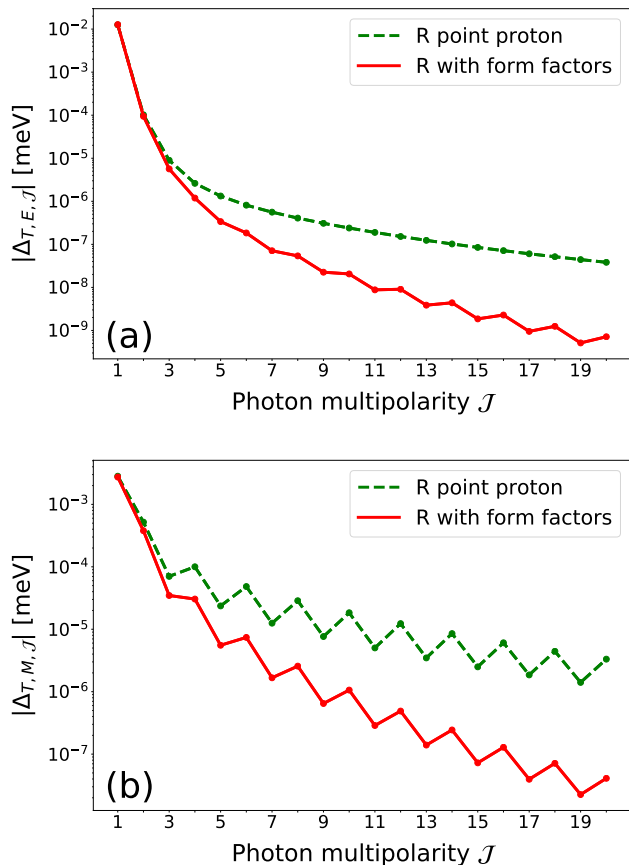


FIG. 4. The absolute value of the (a) transverse Siegert corrections and magnetic transverse corrections (b) plotted as a function of the photon multipolarity \mathcal{J} for μD in the point proton limit and with nucleon form factors.

and $\delta_{\text{pol}}^{\text{NR/R}}$ in the point nucleon limit have excellent agreement ($< 0.15\%$) between the η and η -less methods. However, when nucleon form factors are included, then δ_{Zem}^A and δ_{pol}^A differ by 4% and 2%, respectively, from the η -expansion result. Although these changes appear large, when their contributions are added for δ_{TPE}^A , the difference reduces to 0.2% between the η and η -less results.

V. CONCLUSION

In this work, we have generalized the formalism of Refs. [1, 2] and made it more tractable for the study of the TPE in muonic atoms and obtained what we call the η -less expansion formalism. The calculations are done for both non-relativistic and relativistic cases. We have shown how the elastic terms implicitly included in the more general formalism can be separated from the calculations of the inelastic nuclear contributions. We applied this formalism to muonic deuterium in the non-relativistic limit and full relativistic cases with and without nucleon form factors and compared the results against those obtained from the η -expansion. Compar-

		η -expansion	η -less
Point proton	$\delta_{\text{pol}}^{\text{NR}}$	-1.328	-1.326
	δ_{Zem}^A	-0.359	-0.359
	δ_{TPE}^A	-1.687	-1.685
Point proton	$\delta_{\text{pol}}^{\text{R}}$	-1.308	-1.309
	δ_{Zem}^A	-0.359	-0.359
	δ_{TPE}^A	-1.667	-1.668
R+FF	δ_{pol}^A	-1.248	-1.269
	δ_{Zem}^A	-0.423	-0.406
	δ_{TPE}^A	-1.671	-1.675

TABLE V. A comparison of the results from the η -formalism to the full η -less formalism in the non-relativistic point-proton, relativistic point-proton and relativistic with exact nucleon form factor (R+FF) calculations in units of meV, with $\delta_{\text{TPE}}^A = \delta_{\text{pol}}^A + \delta_{\text{Zem}}^A$. The Coulomb correction $\delta_C^{(0)} = 0.262$ meV from [3], not treated here, has also been added to $\delta_{\text{pol}}^{\text{NR}}, \delta_{\text{pol}}^{\text{R}}, \delta_{\text{pol}}^A$, for comparison

ing the results for $\delta_{\text{pol}}^{\text{NR}}$ in Table V amounts to a difference of only 0.1% between the η -less and η -expansion methods. This difference is from the higher order corrections included in the η -less formalism indicating that without nucleon form factors the nuclear structure calculations are reliable. The inclusion of nucleon form factors into the η -less calculations produces a discrepancy of 4% and 2% for the δ_{Zem}^A and δ_{pol}^A terms, respectively, in comparison to the η -expansion results [3]. For the latter, the form factors are approximated in a low- q expansion and truncated at linear order in q^2 . Since the η -less formalism employs exact nucleon form factors these differences indicate that the linear approximations of the nucleon form factors, used in the η -expansion [3], produce a higher-than-expected systematic uncertainty. However, this low- q truncation uncertainty is removed when their sum δ_{TPE}^A is considered. We found that the calculation of δ_{TPE}^A for muonic deuterium with embedded nucleon form factors is different from the η -expansion by only about 0.2%, which fully justifies the approximations made in the η -expansion for μD . This difference represents the systematic uncertainty of the η -formalism for muonic deuterium which has, for the first time, been rigorously assessed.

Combining with the Lanczos sum rules, the η -less expansion is a promising computational framework that can be applied to muonic atoms with heavier nuclei. This method can systematically compute δ_{TPE}^A to higher orders and with better precision than calculations done in η formalism. Therefore this computational framework will be an important tool for future studies of nuclear structure effects.

VI. ACKNOWLEDGMENTS

The authors would like to thank Nir Nevo Dinur for insightful discussions. This work has been supported by the Cluster of Excellence ‘‘Precision Physics, Fundamental Interactions, and Structure of Matter’’ (PRISMA+ EXC 2118/1) funded by the German Research Foundation (DFG) within the German Excellence Strategy (Project ID 39083149), and by the National Natural Science Foundation of China (Grant No. 11805078).

Appendix A: Analytical $\not\pi$ EFT

In $\not\pi$ EFT at next-to-next-to-leading order, the deuteron wave function is in the S -wave spin-triplet state only [11]. This allows δ_{pol}^A to be calculated analytically. In this section, we show how this approximation can be used to carry out the calculation of the nuclear TPE as outlined in this work. In this formalism, the deuteron wave function is

$$\langle \mathbf{r} | N_0 \rangle = \frac{A_s}{\sqrt{4\pi}} \frac{e^{-\kappa r}}{r}, \quad (\text{A1})$$

where

$$\kappa = \sqrt{2\mu|E_0|}/\hbar, \quad (\text{A2})$$

$$\mu = \frac{m_p m_n}{m_p + m_n} = \frac{m_N}{2}. \quad (\text{A3})$$

Here, $E_0 = -2.224575(9)$ MeV is the deuteron binding energy, $A_s = 0.8845(8)$ fm $^{-1/2}$ is the asymptotic normalization constant and μ is the reduced proton and neutron mass. The summation over intermediate excited states can be performed by introducing plane waves

$$\sum_{N \neq N_0} |N\rangle \langle N| = \int \frac{d^3 k}{(2\pi)^3} |\mathbf{k}\rangle \langle \mathbf{k}| - |N_0\rangle \langle N_0|, \quad (\text{A4})$$

where the nuclear excitation energy is

$$\omega_k = T_k - E_0 = \frac{k^2}{2\mu} + \frac{\kappa^2}{2\mu}. \quad (\text{A5})$$

The matrix elements to evaluate δ_{pol}^A in $\not\pi$ EFT are

$$\langle N_0 | 1 - e^{i\frac{1}{2}\mathbf{q}\cdot\mathbf{r}} | \mathbf{k} \rangle = \sqrt{4\pi} A_s \left[\frac{1}{\kappa^2 + |\mathbf{k} + \frac{1}{2}\mathbf{q}|^2} - \frac{1}{\kappa^2 + k^2} \right], \quad (\text{A6})$$

$$\langle N_0 | 1 - e^{i\frac{1}{2}\mathbf{q}\cdot\mathbf{r}} | N_0 \rangle = A_s^2 \left[\frac{1}{2\kappa} - \frac{2}{q} \tan^{-1} \left(\frac{q}{4\kappa} \right) \right], \quad (\text{A7})$$

$$\langle N_0 | e^{i\frac{1}{2}\mathbf{q}\cdot\mathbf{r}} | N_0 \rangle = \frac{2A_s^2}{q} \tan^{-1} \left(\frac{q}{4\kappa} \right). \quad (\text{A8})$$

These expressions are related to the η -less method in section II B, through a multipole decomposition of the matrix elements. This decomposition is carried out by and introducing the $g_{\mathcal{J}}(k, q)$ functions

$$\frac{1}{\kappa^2 + |\mathbf{k} + \frac{1}{2}\mathbf{q}|^2} - \frac{1}{\kappa^2 + k^2} = \sum_{\mathcal{J}=0} g_{\mathcal{J}}(k, q) P_{\mathcal{J}}(x), \quad (\text{A9})$$

with

$$g_{\mathcal{J}}(k, q) = \frac{2\mathcal{J} + 1}{2} \int_{-1}^1 dx P_{\mathcal{J}}(x) \times \left[\frac{1}{\kappa^2 + k^2 + \frac{1}{4}q^2 + kqx} - \frac{1}{\kappa^2 + k^2} \right]. \quad (\text{A10})$$

Integrating out the angle \hat{k} , we have

$$\int d\hat{k} |\langle N_0 | 1 - e^{i\frac{1}{2}\mathbf{q}\cdot\mathbf{k}} | \mathbf{k} \rangle|^2 = 4\pi A_s^2 \sum_{\mathcal{J}=0} \frac{4\pi}{2\mathcal{J} + 1} g_{\mathcal{J}}^2(k, q). \quad (\text{A11})$$

Combining all of these expressions, the leading order non-relativistic point nucleon corrections are given by

$$\delta_{\text{pol}}^{\text{NR}} = -8\alpha^2 |\phi_{\mu}(0)|^2 \int_0^{\infty} \frac{dq}{q^2} \times \left\{ \sum_{\mathcal{J}=0}^{\infty} \frac{4\pi A_s^2}{(2\mathcal{J} + 1)} \int_0^{\infty} \frac{k^2 dk}{(2\pi)^3} K_{\text{NR}}(q, \omega_k) g_{\mathcal{J}}^2(k, q) - K_{\text{NR}}(q, 0) A_s^4 \left[\frac{1}{2\kappa} - \frac{2}{q} \tan^{-1} \left(\frac{q}{4\kappa} \right) \right]^2 \right\}. \quad (\text{A12})$$

Appendix B: Finite nucleon size corrections in the η -less expansion

In this appendix, we show that when nucleon form factors are included, δ_{pol}^A becomes

$$\delta_{\text{pol}}^A = \Delta_{\omega}^{\text{inel}} + \delta_{Z3}^{(1)} + \delta_{Z1}^{(1)} + \delta_{R3}^{(1)} + \delta_{R1}^{(1)} \quad (\text{B1})$$

where $\delta_{Z3}^{(1)}$ is the third-Zemach moment of the nucleus in Eq. (12), $\delta_{R3}^{(1)}$ is the term defined in Eq. (11) and the terms $\delta_{Z1}^{(1)}$, $\delta_{R1}^{(1)}$ are the finite nucleon size corrections to those terms

$$\delta_{R1}^{(1)} = -\frac{\pi}{3} m_r (Z\alpha)^2 |\phi_{\mu}(0)|^2 \times [\langle Y_{pp}^3 \rangle_{(2)} + \langle Y_{nn}^3 \rangle_{(2)} + 2\langle Y_{np}^3 \rangle_{(2)}], \quad (\text{B2})$$

$$\delta_{Z1}^{(1)} = \frac{\pi}{3} m_r (Z\alpha)^2 |\phi_{\mu}(0)|^2 \times [\langle Z_{pp}^3 \rangle_{(2)} + \langle Z_{nn}^3 \rangle_{(2)} + 2\langle Z_{np}^3 \rangle_{(2)}]. \quad (\text{B3})$$

The terms $\langle Y_{ab}^3 \rangle_{(2)}$ and $\langle Z_{ab}^3 \rangle_{(2)}$ with $(a, b) = (p, p), (n, p), (n, n)$ denote the following integrals

$$\begin{aligned} \langle Y_{pp}^3 \rangle_{(2)} &= \frac{48}{\pi} \int_0^\infty \frac{dq}{q^4} [G_E^p(q^2)^2 - 1] \\ &\times [\langle N_0 | \tilde{\rho}^p(q) \tilde{\rho}^{p,\dagger}(q) | N_0 \rangle - 1], \end{aligned} \quad (\text{B4})$$

$$\begin{aligned} \langle Y_{np}^3 \rangle_{(2)} &= \frac{48}{\pi} \int_0^\infty \frac{dq}{q^4} G_E^n(q^2) \\ &\times [\langle N_0 | \tilde{\rho}^p(q) \tilde{\rho}^{n,\dagger}(q) | N_0 \rangle G_E^p(q^2) - 1], \end{aligned} \quad (\text{B5})$$

$$\begin{aligned} \langle Y_{nn}^3 \rangle_{(2)} &= \frac{48}{\pi} \int_0^\infty \frac{dq}{q^4} G_E^n(q^2)^2 [\langle N_0 | \tilde{\rho}^n(q) \tilde{\rho}^{n,\dagger}(q) | N_0 \rangle - 1], \\ & \quad (\text{B6}) \end{aligned}$$

$$\begin{aligned} \langle Z_{pp}^3 \rangle_{(2)} &= \frac{48}{\pi} \int_0^\infty \frac{dq}{q^4} [G_E^p(q^2)^2 - 1] \\ &\times [|\langle N_0 | \tilde{\rho}^p(q) | N_0 \rangle|^2 - 1], \end{aligned} \quad (\text{B7})$$

$$\begin{aligned} \langle Z_{np}^3 \rangle_{(2)} &= \frac{48}{\pi} \int_0^\infty \frac{dq}{q^4} G_E^n(q^2) \\ &\times [\langle N_0 | \tilde{\rho}^p(q) | N_0 \rangle \langle N_0 | \tilde{\rho}^{n,\dagger}(q) | N_0 \rangle G_E^p(q^2) - 1], \end{aligned} \quad (\text{B8})$$

$$\begin{aligned} \langle Z_{nn}^3 \rangle_{(2)} &= \frac{48}{\pi} \int_0^\infty \frac{dq}{q^4} G_E^n(q^2)^2 [|\langle N_0 | \tilde{\rho}^n(q) | N_0 \rangle|^2 - 1]. \\ & \quad (\text{B9}) \end{aligned}$$

The above expressions correspond to the same expressions $\delta_{Z1}^{(1)}, \delta_{R1}^{(1)}$ as in Ref. [3] in the low- q limit of the nucleon form factors where $G_E^p(q^2) \approx 1 - 2q^2/\beta^2$ and $G_E^n(q^2) \approx \lambda q^2$.

	η -expansion	η -less
$\delta_{Z3}^{(1)}$	0.359	0.359
$\delta_{Z1}^{(1)}$	0.064	0.047
$\delta_{R1}^{(1)}$	0.017	0.016

TABLE VI. A comparison between the nucleon size corrections obtained in the η -less formalism with the approximated nucleon form factors to the η -less expansion results with exact nucleon form factors in units of meV.

Appendix C: Multipole expansion

To compute the expressions in Eqs. (23), (24), and (25), the charge density $\tilde{\rho}(q)$ and current density $\hat{e}_\lambda^\dagger \cdot \tilde{\mathbf{J}}(q)$ are expanded in plane waves as

$$\tilde{\rho}(q) = \sum_{\mathcal{J} \geq 0} \sqrt{4\pi(2\mathcal{J}+1)} i^{\mathcal{J}} C_{\mathcal{J}}(q), \quad (\text{C1})$$

$$\begin{aligned} \hat{e}_\lambda^\dagger \cdot \tilde{\mathbf{J}}(q) &= - \sum_{\mathcal{J} \geq 1} \sqrt{2\pi(2\mathcal{J}+1)} i^{\mathcal{J}} \\ &\times [T_{\mathcal{J}-\lambda}^E(q) + \lambda T_{\mathcal{J}-\lambda}^M(q)]. \end{aligned} \quad (\text{C2})$$

The operators $C_{\mathcal{J}}(q)$ are the Coulomb multipole operators

$$C_{\mathcal{J}}(q) = \int d^3x j_{\mathcal{J}}(qx) Y_{\mathcal{J}}^0(\hat{x}) \rho(\mathbf{x}), \quad (\text{C3})$$

and $T_{\mathcal{J}\lambda}^{E/M}(q)$ are the transverse electric/magnetic tensor operators, respectively, with photon multipolarity \mathcal{J} as in Ref. [30]

$$T_{\mathcal{J}\lambda}^E(q) = \frac{1}{q} \int d^3x [\nabla \times j_{\mathcal{J}}(qx) \mathbf{Y}_{\mathcal{J}\lambda}^E(\mathbf{x})] \cdot \mathbf{J}_c(\mathbf{x}), \quad (\text{C4})$$

$$\begin{aligned} T_{\mathcal{J}\lambda}^M(q) &= \int d^3x \{ j_{\mathcal{J}}(qx) \mathbf{Y}_{\mathcal{J}\lambda}^M(\hat{x}) \cdot \mathbf{J}_c(\mathbf{x}) \\ &+ [\nabla \times j_{\mathcal{J}}(qx) \mathbf{Y}_{\mathcal{J}\lambda}^M(\mathbf{x})] \cdot \mathbf{J}_s(\mathbf{x}) \}. \end{aligned} \quad (\text{C5})$$

The functions $\mathbf{Y}_{\mathcal{J}\lambda}^E(\mathbf{x})$ are the spherical vector harmonics, while $\mathbf{J}_s(\mathbf{x})$ is the nuclear spin current and $\mathbf{J}_c(\mathbf{x})$ is the convection current [31]. Using this expansion, the longitudinal S_L and transverse S_T response functions in Section II B are expanded as sums of multipole functions with photon multiplicities \mathcal{J}

$$S_L(q, \omega) = \sum_{\mathcal{J}=0}^{\infty} S_{L,\mathcal{J}}(q, \omega), \quad (\text{C6})$$

$$S_T^{E/M}(q, \omega) = \sum_{\mathcal{J}=1}^{\infty} S_{T,\mathcal{J}}^{E/M}(q, \omega). \quad (\text{C7})$$

The transverse response function is separated into the sum of electric and magnetic terms

$$S_T(q, \omega) = S_T^E(q, \omega) + S_T^M(q, \omega). \quad (\text{C8})$$

The expressions for each multipole function are

$$\begin{aligned} S_{L,\mathcal{J}}(q, \omega) &= \frac{4\pi}{2J_0 + 1} \sum_{N \neq N_0} |\langle N | C_{\mathcal{J}}(q) | N_0 \rangle|^2 \\ &\times \delta(\omega_N - \omega), \end{aligned} \quad (\text{C9})$$

$$\begin{aligned} S_{T,\mathcal{J}}^{E/M}(q, \omega) &= \frac{4\pi}{2J_0 + 1} \sum_{N \neq N_0} |\langle N | T_{\mathcal{J}}^{E/M}(q) | N_0 \rangle|^2 \\ &\times \delta(\omega_N - \omega). \end{aligned} \quad (\text{C10})$$

In this work, we apply the Siegert theorem to relate the electric transverse multipole functions $S_{T,\mathcal{J}}^E$ to the longitudinal ones through

$$S_{T,\mathcal{J}}^E(q, \omega) = \frac{\omega^2}{q^2} \left[\frac{\mathcal{J} + 1}{\mathcal{J}} \right] S_{L,\mathcal{J}}(q, \omega) + \delta S_{T,\mathcal{J}}(q, \omega), \quad (\text{C11})$$

where $\delta S_{T,\mathcal{J}}(q, \omega)$ is the correction to the Siegert approximation. In Refs. [32, 33] this correction has been shown to be negligible in the low momentum region that dominate the integrals of Eq. (16) and will not be included in this analysis.

In the low- q limit, the Siegert approximated transverse electric response function reduces to only the dipole part with $\mathcal{J} = 1$:

$$S_{T,\mathcal{J}}^E(0, \omega) = S_{T,1}^E(0, \omega) \delta_{\mathcal{J},1} = \frac{2\omega^2}{9} R_D(\omega) \delta_{\mathcal{J},1}, \quad (\text{C12})$$

where $R_D(\omega)$ is the electric dipole function of the nucleus,

$$R_D(\omega) = \frac{4\pi}{2J_0 + 1} \sum_{N \neq N_0} |\langle N || \sum_{i=1}^A \hat{p}_i r_i Y^1(\hat{r}_i) || N_0 \rangle|^2 \times \delta(\omega_N - \omega), \quad (\text{C13})$$

the operators \hat{p}_i are the proton charge projection operators. Because Eq. (C12) is non-zero at $\mathcal{J} = 1$, $q = 0$ and the transverse Kernel is singular at low- q , the dipole contributions in Eq. (24) requires regularization. The seagull term in Fig. 1 removes the singularity of the transverse Kernel for this multipole. Higher electric multipole response functions vanish in the $q \rightarrow 0$ limit and do not require the Seagull term. Similarly, the transverse magnetic response function $S_T^M(q, \omega)$ vanishes in the low- q limit for all multipoles and does not require the regularization term.

-
- [1] R. Rosenfelder, *Nucl. Phys. A* **393**, 301 (1983).
 - [2] W. Leidemann and R. Rosenfelder, *Phys. Rev. C* **51**, 427 (1995).
 - [3] C. Ji, S. Bacca, N. Barnea, O. J. Hernandez, and N. Nevo Dinur, *J. Phys. G* **45**, 093002 (2018).
 - [4] R. Pohl *et al.*, *Nature* **466**, 213 EP (2010).
 - [5] A. Antognini *et al.*, *Science* **339**, 417 (2013).
 - [6] R. Pohl *et al.*, *Science* **353**, 669 (2016).
 - [7] R. Pohl, private communications.
 - [8] A. C. Zemach, *Phys. Rev.* **104**, 1771 (1956).
 - [9] J. L. Friar, *Phys. Rev. C* **16**, 1540 (1977).
 - [10] K. Pachucki, *Phys. Rev. Lett.* **106**, 193007 (2011).
 - [11] J. L. Friar, *Phys. Rev. C* **88**, 034003 (2013).
 - [12] O. Hernandez, C. Ji, S. Bacca, N. N. Dinur, and N. Barnea, *Phys. Lett. B* **736**, 344 (2014).
 - [13] K. Pachucki and A. Wienczek, *Phys. Rev. A* **91**, 040503 (2015).
 - [14] C. E. Carlson, M. Gorchtein, and M. Vanderhaeghen, *Phys. Rev. A* **89**, 022504 (2014).
 - [15] O. Hernandez, A. Ekström, N. N. Dinur, C. Ji, S. Bacca, and N. Barnea, *Phys. Lett. B* **778**, 377 (2018).
 - [16] P. J. Mohr, D. B. Newell, and B. N. Taylor, *Rev. Mod. Phys.* **88**, 035009 (2016).
 - [17] U. Jentschura, A. Matveev, C. Parthey, J. Alnis, R. Pohl, T. Udem, N. Kolachevsky, and T. Hänsch, *Phys. Rev. A* **83**, 042505 (2011).
 - [18] K. Pachucki, V. Patkóš, and V. A. Yerokhin, *Phys. Rev. A* **97**, 062511 (2018).
 - [19] M. Kalinowski, *Phys. Rev. A* **99**, 030501 (2019).
 - [20] C. Ji, N. Nevo Dinur, S. Bacca, and N. Barnea, *Phys. Rev. Lett.* **111**, 143402 (2013).
 - [21] O. J. Hernandez, N. N. Dinur, C. Ji, S. Bacca, and N. Barnea, *Hyp. Int.* **237** (2016).
 - [22] N. N. Dinur, C. Ji, S. Bacca, and N. Barnea, *Phys. Lett. B* **755**, 380 (2016).
 - [23] O. J. Hernandez, The University of British Columbia, Ph.D. Dissertation (2019).
 - [24] N. Nevo Dinur, N. Barnea, C. Ji, and S. Bacca, *Phys. Rev. C* **89**, 064317 (2014).
 - [25] D. R. Entem and R. Machleidt, *Phys. Rev. C* **68**, 041001 (2003).
 - [26] J. L. Friar and G. L. Payne, *Phys. Rev. C* **72**, 014002 (2005).
 - [27] J. L. Friar and G. L. Payne, *Phys. Lett. B* **618**, 68 (2005).
 - [28] S. Binder, A. Ekström, G. Hagen, T. Papenbrock, and K. A. Wendt, *Phys. Rev. C* **93**, 044332 (2016).
 - [29] C. Perdrisat, V. Punjabi, and M. Vanderhaeghen, *Prog. Part. Nucl. Phys.* **59**, 694 (2007).
 - [30] J. Walecka, *Theoretical nuclear and subnuclear physics* (World Scientific, Hackensack, NJ, 2004).
 - [31] W. W. T. Ericson, *Pions and Nuclei* (Oxford, 1988).
 - [32] S. Bacca, H. Arenhövel, N. Barnea, W. Leidemann, and G. Orlandini, *Phys. Rev. C* **76**, 014003 (2007).
 - [33] S. Bacca and S. Pastore, *J. Phys. G* **41**, 123002 (2014).